# Genetic control of neuronal activity enhances axonal growth only on permissive substrates

**Francina Mesquida-Veny[1,2,3,4], Sara Martinez-Torres[1,2,3,4], José Antonio Del Río[1,2,3,4†], Arnau Hervera[1,2,3,4†*]**

[1] Molecular and Cellular Neurobiotechnology, Institute for Bioengineering of Catalonia (IBEC), Barcelona, Spain

[2]Department of Cell Biology, Physiology and Immunology, University of Barcelona, Barcelona, Spain

[3]Network Centre of Biomedical Research of Neurodegenerative Diseases (CIBERNED), Institute of Health Carlos III, Ministry of Economy and Competitiveness, Madrid, Spain

[4]Institute of Neuroscience, University of Barcelona, Barcelona, Spain

[†]These authors share senior authorship

*** Correspondence:**

ahervera@ibecbarcelona.eu

**Keywords: Optogenetics, chemogenetics, regeneration, permissive substrate, neuronal activity.**

## Abstract

Neural tissue has limited regenerative ability, to cope with that, in the recent years a diverse set of novel tools have been used to tailor neurostimulation therapies and promote functional regeneration after axonal injuries. In this report, we explore cell-specific methods to modulate neuronal activity, including opto- and chemogenetics to assess the effect of specific neuronal stimulation in the promotion of axonal regeneration after injury. We found that opto- or chemogenetic modulations of neuronal

activity on both dorsal root ganglia and corticospinal motor neurons increase their axonal growth capacity only on permissive substrates.

## Background

Following injury, damaged axons from the central nervous system (CNS) degenerate and are unable to regenerate, while surviving fibres, have a limited capacity to sprout and to re-establish lost connections, leading to functional impairment [1].

This failure of CNS axons to regenerate after injury is partly attributed to a hostile CNS environment for growth [2–4]. The injury site is rich in growth inhibitory proteins including myelin-associated glycoproteins, and chondroitin sulfate proteoglycans (CSPG) while lacking trophic support for axon regeneration [5–7]. The limited intrinsic regenerative capacity of adult CNS axons also contributes to the failure of axon regeneration after injury [8–10]. Yet, in the last years there have been several studies approaching different aspects of the CNS physiology to both boost the intrinsic regrowth capacity and overcome the extrinsic inhibition [11, 12].

During development, when CNS neurons still retain their intrinsic ability to regenerate after axotomy [13], neuronal activity critically determines their connectivity, particularly onto spinal targets [14]. In this direction, neuronal activation has also been explored to try to increase the intrinsic capacity for axon regeneration as well as overcome the extrinsic inhibition. Practically, electrical stimulation has been shown to enhance regeneration of sensory axons after peripheral nerve or dorsal columns injury [15, 16] and sprouting of cortical axons into contralateral spinal cord gray matter after pyramidotomy [17–19].

In order to gain insight on the actual mechanisms underlying these improvements, specifically and remotely activating neurons through opto- and chemogenetics, has become the state-of-the-art approach for tailored activity modulation [20, 21].

In this direction, the current study explores the therapeutic potential of modulating neuronal activity of sensory (dorsal root ganglia (DRG)) and motor descending (corticospinal motor neurons (CSMN)) neurons, via opto- and chemogenetic stimulation in regulating axonal growth after injury.

We found that specific neuronal stimulation induced increased axonal growth capacity both *in vitro* and *in vivo*, and both in sensory and motor neurons, but only when in presence of permissive and trophic environments. Opto- or chemogenetic stimulation did not overcome the inhibitory signalling induced by molecules such as myelin-associated glycoproteins and CSPGs.

## Methods

### *Mice*

B6.Cg-Tg(Thy1-COP4/EYFP)18Gfng/J (Thy1-ChR2) (Jackson Laboratories) [22] or wild type (WT) C57BL/6J mice (Charles River Laboratories) ranging from 6-10 weeks of age were used for the experiments and were randomly divided into the different experimental groups. Mice were anaesthetized with isoflurane (5% induction, 2% maintenance) during surgeries. For DRG neuronal cultures adult Thy1-ChR2 mice were used. Embryonic day 16.5 (E16.5) OF1 pregnant females were purchased from Charles River Laboratories, and the embryos were used for neuronal cortical cultures. All procedures were approved by the Ethics Committee on Animal Experimentation (CEEA) of the University of Barcelona (CEEA approval #276/16 and 141/15).

### *Dorsal root ganglia (DRG) neuronal culture*

DRGs from adult Thy1-ChR2 mice were dissected, washed in cooled Hank's balanced salt solution (HBSS; ThermoFisher Scientific), and enzymatically digested (5mg/ml Dispase II (Merck) and 2.5mg/ml Collagenase Type II (ThermoFisher Scientific) in DMEM (ThermoFisher Scientific)) for 45min at 37ºC. Next, the DRGs were resuspended in DMEM:F12 (ThermoFisher Scientific) media supplemented with 10% heat-inactivated Fetal Bovine Serum (FBS; ThermoFisher Scientific) and 1x B27 (ThermoFisher Scientific) and were mechanically dissociated by pipetting. After centrifugation, the resulting single cells were resuspended in culture media (DMEM:F12 media with 1x B27 and penicillin/streptomycin (P/S; ThermoFisher Scientific)) and plated in glass-coverslips (3000-4000 cells/well) or in microfluidic devices (20.000cells/device) pre-coated with 0.1mg/ml poly-D-lysine (2h, 37ºC; Merck) and 2µg/ml laminin (over-night (O/N); ThermoFisher Scientific) at RT (room temperature)). An additional incubation with 5, 10 or 20 µg/ml CSPGs (Merck) was performed (2h at 37ºC) in growth-inhibitory substrate experiments. Cells were allowed to grow for 24h or for 8 days (in the case of microfluidic devices) at 37ºC in a 5% $CO_2$ atmosphere.

***Neuronal cortical culture***

E16.5 WT mice embryos were used for neuronal cortical cultures. Brains were extracted, washed in cooled 0.1M phosphate-buffered saline (PBS; ThermoFisher Scientific) containing 6.5 mg/ml glucose (Sigma Aldrich) (PBS-glucose) and the meninges excised. Both cortical lobes were dissected, sliced in a McIlwain II tissue chopper (Capdem Instruments) and trypsinized for 15 min at 37ºC. The suspension was inactivated with Normal Horse Serum (NHS; ThermoFisher Scientific), incubated with 0.025% DNAse (Roche) PBS-glucose for 10 min at 37ºC and mechanically dissociated. Single cells were spun down and resuspended in Neurobasal™ (ThermoFisher Scientific) medium supplemented with 2mM glutamine (ThermoFisher Scientific), P/S, 6.5mg/ml glucose, $NaHCO_3$ (Merck), 1x B27 and NHS 5% and plated in poly-D-lysine (0.1mg/ml) pre-coated microfluidic devices (see below) (150.000cells/device) or in glass-bottom plates (200.000cels/plate). One day after seeding, culture

media was changed, and NHS was excluded from the new media. Cells were maintained at 37ºC in a 5% CO2 atmosphere and culture media was changed every two days.

### *Microfluidic devices*

The design used for microfluidic devices were a modification of a previously published device[23, 24]. One of the devices consists in 4 reservoirs of 7mm diameter, connected in pairs by a longitudinal compartment (cell body and axonal compartments) which are in turn interconnected by 100 microchannels (10µm x 10µm x 900µm). The other used device presented a similar design and included a perpendicular channel to the microchannels, located at the center of these. The masters were produced using standard photolithography techniques at IBEC Microfab Space. Poly(dimethylsiloxane) (PDMS; Dow) was used to prepare the devices by soft lithography, which were subsequently attached to glass bottom dishes using oxygen plasma treatment.

In the first device, cortical neurons were seeded in one of the larger compartments (cell body compartment) and allowed to extend their axons across the microchannels. In the case of the second device, which was used with DRG neurons, neurons were seeded in the central channels. Vacuum aspiration in the axonal compartment allowed complete axotomies [24].

### **In vitro *lentiviral production and infection***

LV-EF1α-hChR2(H134R)-EYFP-WPRE (LV-ChR2) produced in our laboratory were used to introduce ChR2 expression in primary cortical neurons. For LV production, 293-FT (ATCC) cells were simultaneously co-transfected with three plasmids: pMD2.G (VSV-G envelope expressing plasmid), psPAX2 (lentiviral packaging plasmid), and pLenti-EF1α-hChR2(H134R)-EYFP-WPRE (transfer plasmid) in Opti-MEM (ThermoFisher Scientific) using Lipofectamine 2000 Transfection Reagent (ThermoFisher Scientific). Transfection media was changed for culture media (Advanced DMEM

(ThermoFisher Scientific) supplemented with 10% FBS, 1% P/S and 0.5% glutamine) 6h after. Media was recovered at 48h and 72h post-transfection, filtered and centrifuged at 1200g to remove debris. The supernatant was then centrifuged at 26.000rpm for 2h at 4ºC in a Beckman conical tube containing a sucrose cushion (20%) for purification, ant the viral pellet was finally resuspended in PBS-1% BSA. Cortical neurons were infected at 4 days *in vitro* (DIV) for 24h, and high levels of YFP fluorescence could be observed at 7DIV, indicating positive infection.

**In vitro *optogenetic stimulation***

Thy1-ChR2 DRG neurons or cortical neurons infected with LV-ChR2 were used for *in vitro* optogenetic stimulation experiments. A 470nm emission LED array (LuxeonRebelTM) under the control of a Driver LED (FemtoBuck, SparkFun) of 600mA and a pulse generator PulsePal (OpenEphys)[25] was used to deliver blue light to neuronal cultures. The optogenetic stimulation protocol consisted in 1h of illumination at 20Hz of frequency with 5ms-45ms pulses, in 1s ON-1s OFF periods. In the case of DRG neurons, stimulation was applied 2h after seeding. For cortical neurons, two different stimulation time-points after the axotomy were assessed: 30 min after axotomy and 6h after axotomy. To assess neuronal activation, neurons were fixed at the end of the stimulation. Uninjured cortical neurons were stimulated in this experiment.

**In vitro *chemogenetic stimulation***

10µM CNO (Tocris) was added to DRG cultures 6h after axotomy and left in the media until fixation (24h after the axotomy).

***Corticospinal tract and dorsal columns axotomy***

A fine incision to the skin between the shoulder blades of anaesthetized mice and subsequent muscle removal allowed thoracic vertebral column exposure. A T9 laminectomy was performed, and the dura

mater was excised. In corticospinal tract injuries, two thirds of the spinal cord approximately were severed laterally with a scalpel. In dorsal column axotomies (DCA), a dorsal hemisection was conducted with fine forceps.

***Sciatic nerve crush (SNC)***

The sciatic nerve was exposed after a small incision on the skin over the posterior hindlimb and blunt dissection of the gluteus maximus and the biceps femoralis. Fine forceps were used to carefully compress the nerve orthogonally 2x10s. Animals were allowed to recover for 24h, when were then sacrificed and the sciatic nerve and the sciatic DRGs (L4, L5, L6) were dissected and processed.

**In vivo *optogenetic stimulation***

An optic fiber cannula (1.25mm, 0.22 NA; Thorlabs) was implanted in the motor cortex (M1) of Thy1-ChR2 transgenic mice by stereotaxic surgery (–1mm antero-posterior (AP), 1.5mm lateral to Bregma, 0.5mm deep, (hind limb innervation region)) prior to injury and was fixed to the cranium with screws and dental cement. Correct placement of the cannula was tested for each animal by assessing the induction of unidirectional rotatory locomotion caused by unilateral optical stimulation of the motor component of the hind limb; animals that did not show this response were excluded from the study. At 7 days post-injury (DPI) animals started receiving daily optogenetic stimulations consisting in 1h of illumination with 470nm blue light, at 10Hz of frequency with 10ms pulses, in 1sON-4sOFF periods, for 5 consecutive days, 2 resting days followed by 5 more days. The illumination was delivered through the optic fiber cannula which was coupled to a 470nm wavelength LED source (M470F3, Thorlabs) controlled by a pulse generator (Pulse Pal) [25]. The control group went through the same procedures than the experimental group without receiving illumination.

**In vivo *chemogenetic stimulation***

The commercial AAV5-hSynhM3D(Gq)-mCherry or the control virus AAV5-hSyn-mCherry (Addgene) were injected into the sciatic nerve of C57BL/6J mice (1µL/sciatic nerve) 4-5 weeks before the experiment. For chemogenetic stimulation, the animals received two daily intraperitoneal (i.p.) injections of 5mg/kg CNO (Tocris). After DCA, injections were delivered starting from 3DPI and lasted 7 consecutive days. In the case of SNC, the injections were given prior to injury: from 3 days pre-injury to the same day of the injury (in total 4 days of chemogenetic stimulation).

***Behavioural assessment of sensorimotor function***

Sensorimotor deficits and recovery were evaluated using the gridwalk and the BMS (Basso Mouse Scale) tests at -1, 1, 7, 14, 21, 28 and 35 DPI for CST injuries and at -1, 1, 3, 7, 10, 21 and 28 DPI for DCA. During the gridwalk animals were recorded while walking three times on a grid of 1 x 1 cm squares (total longitude of the grid: 50cm). The number of missteps in relation to the total number of steps was blindly quantified. In BMS evaluations mice were allowed to freely move in an open field and a score was assigned to each of them according to the BMS scale[26]. In brief, this scale grades from 0 to 9 the locomotor capacity of the hind limbs depending on several aspects such as ankle movement, paw placing and position or stepping.

***Tracing of injured spinal cords***

A fluorescent tracer (10% Dextran-Alexa 594, 10.000MW, ThermoFisher Scientific) was injected with a stereotaxic frame (KOPF) into the motor cortex of animals with injured CST at 35DPI using the fibre optic cannula hole, in order to trace the stimulated CST. The tracer was injected at 0.2 µl/minute for a total of 1 µl, adding 5 more minutes at the end to avoid liquid spillage. 5 days were waited before sacrifice, to allow the tracer to be reach the axonal terminations

***Immunocytochemistry (ICC)***

For immunocytochemistry (ICC), cells were fixed with 4% paraformaldehyde (PFA) 15 min on ice, washed and incubated in blocking solution (1% Bovine serum albumin (BSA), 0,25% Triton X-100 (0,25% Tx) in 0.1M PBS) for 1h at RT. Primary antibody (βIII tubulin (Tuj1, 1:1000, BioLegend), c-Fos (1:200, Cell Signaling), ChR2 (1:500, Progen), mCherry (1:500, Abcam) GFP (1:500, ThermoFisher Scientific) was added to the cells in blocking solution and incubated O/N at 4ºC. After washing, the cells were incubated 1h at RT with Alexa-Fluor-conjugated secondary antibodies (568 goat and 488 goat and donkey) and Hoechst (Sigma Aldrich).

***Tissue processing for immunohistochemistry***

Anaesthetized mice were transcardially perfused with ice-cold 4% paraformaldehyde (PFA) and the spinal cord, the brain or the DRGs were dissected and allowed to post-fix in 4% PFA for 24h at 4ºC. In peripheral experiments the sciatic nerves and the DRGs were directly dissected, as perfusion was not needed, and allowed to fix in 4% PFA for 2h on ice. Fixed tissues were cryoprotected in 30% sucrose in PBS for 24h at 4ºC, brains were then directly frozen and sliced at 30 µm with a freezing microtome (2000R Leica), while spinal cords and DRGs were embedded in tissue freezing medium (OCT, Sigma Aldrich), frozen and 18 µm or 10 µm slices respectively were obtained using a cryostat (CM 1900 Leica) and directly mounted. For whole mount stainings cryprotection was not needed, instead tissues were kept in 0.1M PBS.

***Immunohistochemistry (IHC)***

Prior to IHC, brain slices were maintained in cryoprotection solution (30% glycerol, 30% ethylene glycol, 40% PBS). Brain IHCs were performed directly on free floating slices. Slices were blocked for 1h at RT (10% FBS, 0.5% Tx, 0.2% gelatine, 0.2M glycine in 0.1M PBS) and incubated with primary antibody O/N at 4ºC (5% FBS, 0.5% Tx, 0.2% gelatine in 0.1M PBS; GFP (1:500, ThermoFisher

Scientific). Slices were then repeatedly washed with PBS-0.5% Tx, incubated with secondary antibodies (Alexa Fluor 488 donkey; ThermoFisher Scientific) and Hoechst (Sigma Aldrich).

IHCs were performed directly on spinal cord or DRG preparations. Slides were blocked for 1h at RT (Blocking solution: 8% BSA, 0.3% Tx in TBS) was added and incubated for 2h at RT, followed by O/N incubation of primary antibody (GFAP (1:500, Dako); cFos (1:200, Cell Signaling); NFH (1:200; Abcam)) in 2% BSA, 0.2% Tx in TBS at 4ºC. Secondary antibodies (Alexa Fluor 488 donkey and goat and 568 goat; ThermoFisher Scientific) and Hoechst were added after washing with TTBS and incubated 1h at RT.

Whole-mount IHCs were performed for sciatic nerves. Blocking solution (8% BSA, 1% Tx and 1/150 mαIgG (Fabs) in TBS) was added and incubated for 2h at RT, followed by 3 O/N of primary antibody incubation (SCG-10 (1:1000, Novus Biologicals) in 2% BSA, 0.3% Tx in TBS at 4ºC. Secondary antibodies (Alexa Fluor 488 donkey) were added after washing with TTBS and incubated 1 O/N at 4ºC.

Each preparation was subsequently mounted in Mowiol$^{TM}$ (Sigma Aldrich).

***Fluorescence intensity analysis***

To measure c-Fos intensity, DRG neurons were immunostained for c-Fos and ChR2 and imaged at 40x magnification with an Olympus microscope IX71 using an Orca Flash 4 (Hamamatsu Photonics). Only ChR2$^{+}$ cells were selected for this analysis. About 20 cells per well were analysed. The nuclei of the cells were selected, and its mean c-Fos intensity determined by subtracting the corresponding background value to the integrated density (Corrected total cell fluorescence; CTCF), measured using ImageJ$^{TM}$.

***Neurite and axonal length analysis***

Images were taken at 10x magnification with an Olympus microscope IX71 using an Orca Flash 4 or a CX50 Olympus camera. TUJ1, mCherry or GFP was used to immunolabel neurites and axons. For DRG neurite analysis, three fields per well were analysed and the average neurite length per cell was obtained. Small diameter (<35µm) neurons were excluded from the analysis. In microfluidic devices, the percentage of regenerating axons normalized to the total number of axons reaching the axonal compartment was determined. For cortical neuron cultures, 8-9 fields per device were analyzed. Either average axon length or total area covered by axons was quantified. Neurite-J plugin in ImageJ™ software was used for neurite and axonal measurements [27]. Area measurements were measured using ImageJ™ software.

***Sprouting quantification***

To quantify the number of sprouting axons before and after the lesion, we measured the tracer fluorescence intensity on sections at 0,5mm pre-injury and post-injury level. The spinal cord section images were divided in two different ROIs corresponding to grey matter and white matter for analysis.

Spinal cord sections of stimulated and non-stimulated Thy1-ChR2 mice at 500µm rostral to the lesion core were obtained using a confocal microscope (LSM 800, AxioCam 503c; Zeiss) at 10x magnification. The number of double positive axons for Dextran-Alexa 594/ChR2-YFP in the grey matter at different distances from the CST in the same section was computed and normalized to the number of Dextran-traced CST.

***Nerve regeneration analysis***

Regenerating sensory axons were immunolabeled with SCG10. Whole mount preparations were imaged with a confocal microscope (LSM 800, AxioCam 503c; Zeiss) at 5x magnification. 6-8 tiles and 10-15 slices were obtained per nerve and the Blue Zen™ and ImageJ™ softwares were used to

reconstruct the nerve and obtain a Maximum Intensity Z-projection. The crush site was determined by phase contrast images, the number of regenerating axons at several distances from the crush was determined.

### *Statistical analysis*

Prism 6.0 (GraphPad™ Software) was used for statistics and graphical representation. Plotted data shows mean±s.e.m (standard error of the mean). Normality was determined with Shapiro-Wilk test. Significant differences are indicated by arterisks (*$p < 0.05$; **$p < 0.01$; ***$p < 0.005$; ****$p < 0.001$). ANOVA followed by Bonferroni post hoc test or Student's t-Test were used in normal distributions as opposed to Mann-Whitney or Kruskal-Wallis tests as non-parametric tests for samples that did not meet normality.

## Results

### *Optogenetic stimulation of DRG neurons increase their axonal growth in vitro*

We first sought to determine if optogenetic activation of adult DRG neurons could enhance axonal growth *in vitro*. Adult dissociated Thy1-ChR2 DRG neurons were optically stimulated and allowed to grow for 24h.

Optical stimulation effectively increased neuronal activity in DRG neurons, as displayed by the increased levels of c-Fos staining after stimulation (49627±4373 a.u. of nuclear CTCF intensity for stimulated DRGs versus 33897±3212 a.u. of nuclear CTCF intensity for non-stimulated; $p$=0.0058 Student's t-Test) (Fig 1A-B)

Optically stimulated neurons showed increased neurite outgrowth (4053±433.1µm) after 24h of culture when compared to non- stimulated ones (2029±647.7µm; $p$=0.0267 Student's t-Test) (Fig 1C-D)

***Chemogenetic stimulation of DRG neurons improve their regenerative capacity after in vitro axotomy and sciatic nerve crush***

We then wanted to test if this increased growth capacity also translated in regenerative capacities after axotomy. To this aim we first evaluated regenerative capacity of DRG neurons *in vitro* using microfluidic assisted axotomy and chemogenetic stimulation. DRG neurons were seeded in custom microfluidic devices as previously described, and hM3Dq or mCherry expression was induced by infection with AAVs. Axons were allowed to grow for few days through the microchannels until they reached the axonal chamber, and we then performed a vacuum assisted axotomy. CNO was administered 6 hours after axotomy. Chemogenetic stimulation resulted in axonal regeneration ($p$=0.0165; Student's t-Test) when compared to non-stimulated mCherry controls (Fig 2A-B).

We then wanted to determine if the *in vitro* results in fact translated to enhanced axon regeneration *in vivo* after PNS injury. Due to the difficulty to apply light for long periods of time in awake animals in the DRGs, we used chemogenetics for activity control. We first wanted to determine if DRGs were transduced *in vivo*. AAV5-hSyn-mCherry or AAV5-hSyn-hM3Dq-mCherry were carefully injected into the sciatic nerve and mCherry expression was examined 4-5 weeks later. Both vectors transduced DRG neurons with similar efficiency (~35% of total DRG neurons; ~65% of large diameter (>35µm) neurons (Supp Fig 1A-B). mCherry expression was mainly localized in the soma of large diameter $NFH^+$ DRG neurons (Supp Fig 1C).

To verify the activation of DRG neurons *in vivo* after chemogenetic stimulation, we performed cFos staining 1h after CNO administration, showing increased cFos signal only in hM3Dq animals compared to mCherry controls (Fig 2B).

To assess the effects of neuronal activity on PNS regeneration, animals received 2 daily injections of 5mg/kg CNO 3 days before performing a bilateral SNC to guarantee four consecutive stimulation days

(Fig 2D). 24h after injury hM3Dq stimulated animals showed increased number of regenerating sensory axons ($SCG10^{+}$) at further distances (>750µm) when compared to mCherry controls. The two-way ANOVA showed a significant effect of the distance ($p< 0.0001$) and stimulation ($p=0.0145$) as well as their interaction ($p=0.0101$). At 750µm from the injury stimulated animals showed 27.67±4.19 axons versus 12.78±3.34 axons on non-stimulated animals ($p=0.0694$ Bonferroni post Hoc test), at 1000µm from the injury stimulated animals showed 21.56±3.72 axons versus 6.44±1.43 axons on non-stimulated animals ($p=0.0163$ Bonferroni post Hoc test), at 1250µm from the injury stimulated animals showed 14.89±3.12 axons versus 3.11±1.14 axons on non-stimulated animals ($p=0.0261$ Bonferroni post Hoc test), and at 1500µm from the injury stimulated animals showed 8.56±1.81 axons versus 1.56±1.06 axons on non-stimulated animals ($p=0.0259$ Bonferroni post Hoc test) (Fig 2D-E).

***Optogenetic stimulation of cortical neurons does not improve the sensorimotor performance after SCI***

We then wanted to test if this increased regeneration capacity also was present in the CNS neurons. To this aim we first evaluated regenerative capacity of cortical neurons *in vitro* after optogenetic stimulation. Embryonic cortical neurons were seeded in custom microfluidic devices as previously described, ChR2 was induced by infection with LV-ChR2 (Fig 3A), and activation of neurons upon stimulation was assessed by cFos staining immediately after stimulation (Fig 3B). Axons were allowed to grow for few days through the microchannels until they reached the other chamber, when a vacuum assisted axotomy was performed. Optogenetic stimulation of cortical neurons decreased the axonal regrowth when stimulated 30 minutes after the axotomy Fig 3C). In contrast, 6 hours after axotomy, optogenetic stimulation resulted  increase in axonal regrowth when compared to non-stimulated ones ($p=0.0056$; Mann-Whitney test; Fig 3D-F). To control the intrinsic effect of blue light on neuronal growth, we applied the light stimulation pattern on non-stimulated (GFP controls) embryonic cortical neurons and observed no difference in axonal growth (Fig 3E).

To test if these results further translated to a better motor performance after SCI *in vivo*, we implanted optic fibre cannulas on Thy1-ChR2 animals, that have the cortical expression of ChR2 predominantly concentrated in the layer V, where corticospinal motor projecting neurons lay (Supp. Fig 2A). After recovery, animals were subjected to a CST axotomy, and optical stimulation was performed daily from day 7 after injury (Fig 4A). Stimulated animals did not show any improvement in their motor performance on the Gridwalk (Fig 4B) or the BMS (Fig 4C) when compared to non-stimulated controls. For each test evaluated, the two-way ANOVA showed a significant effect of the time (BMS $p<0.0001$; Gridwalk $p<0.0001$) but neither from the stimulation (BMS $p=0.7201$; Gridwalk $p=0.1308$) nor from their interaction (BMS $p=0.9905$; Gridwalk $p=0.0707$). In all tests, non-significant changes were observed for each timepoint when compared stimulated versus non-stimulated mice (Bonferroni multiple comparisons test).

These results indicate that embryonic CNS neurons have the ability to increase their axonal growth capacity *in vitro* when stimulated, but there are inhibitory signals in the CNS injury that block this regeneration *in vivo.*

***Chemogenetic stimulation of DRG neurons does not improve their sensorimotor performance after SCI***

To test whether the lack of in vivo functional recovery was due to an intrinsic inability to regenerate from corticospinal neurons or the presence of an extrinsic inhibitory signal in the CNS injury, we tested the effects of chemogenetic stimulation on DRG neurons after a dorsal hemisection *in vivo.* Similarly, to what was done for the PNS injury, AAV5-hSyn-mCherry or AAV5-hSyn-hM3Dq-mCherry were carefully injected into the sciatic nerve to induce its expression on the DRG (Supp Fig 1A-C). 4-5 weeks later animals were subjected to a dorsal hemisection, and 3 days after injury animals received 2 daily injections of CNO (5mg/kg b.w.) for 7 days (Fig 4 D). As observed for the cortical stimulation,

329 stimulated animals did not show any improvement in their motor performance on the Gridwalk (Fig
330 4E) or the BMS (Fig 4F) when compared to mCherry-veh, mCherry-CNO or hM3Dq-veh controls.
331 For each test evaluated, the two-way ANOVA showed a significant effect of the time (BMS $p<0.0001$;
332 Gridwalk $p<0.0001$) but neither from the stimulation (BMS $p=0.2289$; Gridwalk $p=0.0694$) nor from
333 their interaction (BMS $p=0.3614$; Gridwalk $p=0.0785$). In all tests, no significant changes were
334 observed for each timepoint when compared stimulated versus non-stimulated mice (Bonferroni
335 multiple comparisons).

336

337 These results suggest the presence of inhibitory cues after CNS injury that could be blocking the
338 regeneration induced by neuronal stimulation. In contrast after PNS injury where no inhibitory
339 environment is present stimulation did induce enhanced growing capacities.***Optogenetic stimulation***
340 ***of DRG neurons increase their axonal growth in vitro, only on permissive substrates***

341 To further assess the impact of CNS inhibitory signals in the activity-induced increased axonal growth,
342 we cultured adult DRG neurons in both permissive (Laminin) and different concentrations of inhibitory
343 (CSPG) substrates and subjected them to optogenetic stimulation.

344 As previously observed (Fig 1C-D), optogenetic stimulation increased the neurite outgrowth in
345 permissive substrates (3761±290.8µm for stimulated DRGs versus 2735±162.9µm for non-stimulated
346 DRGs), but not on neurons seeded at any concentration of CSPGs, including the 5µg/ml concentration,
347 that did not reduce basal growth, where optogenetic stimulation did not produce any change in neurite
348 outgrowth (Fig 5A-B), the two-way ANOVA did not show a significant effect from the stimulation
349 ($p=0.4785$), but it did show a significant effect of the substrate ($p<0.0001$) and their interaction (
350 $p=0.0398$), highlighting the blockage of the stimulation effects in the presence of CSPGs.

***Optogenetic stimulation of corticospinal motor neurons increases prelesion sprouting but does not induce regeneration across the lesion.***

Since activity dependant therapies have been shown to increase lateral sprouting and plasticity [17–19, 28–30], we sought to investigate if our stimulation paradigm increased the sprouting of injured axons before the lesion. To this aim, we analysed the spinal cords of stimulated Thy1-ChR2 mice after tracing their corticospinal tracts. Interestingly, we found that optogenetic stimulated animals did show more axonal tracing in the grey matter (33.60±1.13 a.u. of CTCF intensity for stimulated animals versus 23.27±0.89 a.u. of CTCF intensity on non-stimulated animals; $p$=0.0015 Student's t-Test) in segments before (-0.5mm) the injury, but not beyond (+0.5mm) the injury (14.61±1.21 a.u. of CTCF intensity for stimulated animals versus 12.80±0.47 a.u. of CTCF intensity on non-stimulated animals; $p$=0.30328 Student's t-Test) (Supp Fig 2B-C). Additionally, we also quantified the number of sprouted axons in the grey matter as a ratio from traced CST axons (in order to normalize the tracing efficiency between animals). Interestingly we found that stimulated animals showed a significantly higher percentage of traced sprouts up until 400µm ventrally and laterally from the CST. The two-way ANOVA showed a significant effect of the distance ($p$<0.0001), the stimulation ($p$=0.0401) as well as their interaction ($p$=0.0013). These findings suggest that the positive effects of modulation of the activity on the axonal regrowth are inhibited by CNS inhibitory signals present in the injury.

## Discussion

Neuronal activity-triggered plasticity is commonly recognized as the main component of recovery in current activity-based therapies [31, 32], however, this is mainly built on therapies that use exercise or electrical stimulation to induce neuronal activity (as in [17–19, 28–30]). Even so, even though these approaches increase neuronal activity, they do so without cellular specificity, hindering the identification of underlying cellular and molecular mechanisms induced by neuronal activity itself.

Taking advantage of the cellular specificity of optogenetics and chemogenetics [20, 21] we performed different experiments to assess the specific cellular effects of neuronal activity on axonal growth using different *in vitro* and *in vivo* neuronal models.

Consistent with previous works [23, 33–35], we showed that increasing neuronal activity on DRG sensory neurons enhanced axonal growth in non-inhibitory *in vitro* and *in vivo* peripheral injury models. Additionally, and still accordingly to previous studies [36], we also demonstrated these effects in embryonic cortical cells *in vitro,* highlighting the presence of similar mechanisms among different neuronal types.

It is important to mention that before the achievement of these results, a fine tuning of the stimulation protocol was needed, as axonal growth capacities showed to be highly dependent on the timing after injury and the pulse frequency during the stimulation (data not shown), highlighting the fact that neuronal activity needs, not only to be stimulated, but to be finely regulated in order to promote the desired outcomes. For instance, high frequency stimulations (>20Hz in 1 second trains, or >10Hz in continuous stimulation) reduced the axonal growth *in vitro,* and induced seizures *in vivo*. This has also been emphasized in previous studies indicating activity-dependant effects on gene expression [37–39] and plasticity (reviewed in [40]).

Meanwhile, timing of stimulation after injury seems to be very relevant as well, as stimulating 30 min after axotomy results in reduction of axonal growth compared to non-stimulated controls. This might be caused by the ionic imbalance generated by membrane disruption after axonal injury, that leads to exaggerated $Ca^{2+}$ influx. Membrane sealing and restoring the ionic balance and permeability occurs early after injury, but maintaining neuronal depolarization during this period leads to the activation of some voltage gated cation channels that have been shown to inhibit growth [15, 41, 42] In accordance, little changes in the stimulation patterns might lead to opposed effects, therefore we used optogenetics

whenever possible as our method of choice to stimulate activity since it allowed us a higher temporal resolution [43]. Nonetheless, the anatomical setting of the DRGs impeded the implantation of a permanent optic fiber canula, and therefore did not allow us to perform awake stimulations, as this would have compromised the wellbeing of the animals, therefore, we opted for a chemogenetic approach for *in vivo* DRG stimulation. Effectively, this method rendered similar results on neurons as those observed *in vitro* with optogenetics, resulting in enhanced regeneration. For this experiment we delivered the chemogenetic agonist (CNO) before the injury (as a preconditioning to allow enough stimulation days in this setting), leading to similar effects as those observed in previous studies using enriched environment [44] or electrical stimulation [15, 16, 45] as a preconditioning.

Since our *in vitro* and PNS injury results have shown comparable regeneration outcomes than electrical stimulations [46–48], we believe that neuronal activity itself might be responsible, at least partially, of these effects on axonal growth.

However, when we tested this paradigm in an *in vivo* model of SCI, we found that optogenetic stimulation of spinal-projecting cortical neurons did not promote the expected functional recovery after SCI, contrarily to what other studies observed using electrical stimulation [17–19], or exercise [29, 30, 49] showed.

We then focused on clarifying whether our model did not induce any kind of axonal regeneration, or it did, but was insufficient to promote recovery. In that sense, an *in vivo* CNS model of injury implies the presence of a number of factors absent in our previous experiments, including both the presence of an intrinsic lack of regenerative capacity as well as the presence of extrinsic inhibitory substrates for regeneration [9, 50, 51]. Accordingly, when we performed further histological characterization together with complementing *in vitro* experiments, we found that stimulated neurons displayed increased axonal growth in permissive substrates (laminin), but not in growth inhibitory substrates

(CSPGs), and stimulated neurons showed an increased amount of growth and sprouting in the rostral vicinity of the injury, especially in the grey matter of the SC, but not caudally across or beyond the injury. While we cannot exclude that the lack of regeneration across the injury might be due, at least in part, to the intrinsic low regenerative capacity of corticospinal neurons, our data suggests that neuronal activity stimulates the axonal growth capacity of these neurons, as seen in embryonic cortical neurons *in vitro*, through a mechanism that cannot overcome the repressive signalling of growth-inhibitory molecules, such as CSPGs. Additionally, *in vivo* injured neurons when stimulated start growing through uninjured areas of the SC, similarly to what is described in other studies with classical stimulation approaches [17–19], where injured and uninjured axons grow axonal processes searching for spared intraspinal circuitry, these new connections will eventually restore the injured connections through neuronal plasticity, bypassing the injury [52]. Interestingly, classical non-specific stimulations such as epidural electrical stimulation or rehabilitation lead to stimulation of intraspinal circuits, involving spinal interneurons and motoneurons, this stimulation in turn promotes the reorganization and activation of this circuitry [53]. Whether the lack of these functional effects with our paradigm was due to a shorter stimulation period, or that it lacked the direct stimulation of this intraspinal circuitry and thus not inducing the plasticity needed, remains still unanswered. However, a recent study also observed a blockage of activity-induced axonal growth in the presence of inhibitory-substrates after cellular specific stimulation [54]. In this study, functional recovery after SCI was only achieved after combining chemogenetic stimulation and ChABC administration (a CSPG degrading enzyme) [54], surprisingly functional recovery was only achieved after 6 weeks of continuous combined treatment. In contrast to both this work and our results, both chemogenetic stimulation and visual stimulation induce functional regeneration after optic nerve crush, a CNS injury model [55]. Importantly however, the expression of the different chemogenetic receptors in this study was induced by intravitreal injection of the vectors, meaning that retinal interneurons, including amacrine and bipolar cells, will most likely be expressing the channels and be subjected to stimulation upon agonist administration.

This paradigm resembles to that of electrical stimulation, considering activation of this retinal interneurons might be inducing neuronal plasticity that facilitates functional recovery.

There is plenty of evidence that neuronal activity itself is key in promoting regeneration and recovery, however, the presence of growth inhibitory substrates in the injured CNS limits the success of activity-based therapies. In line with this, combining functional rehabilitation or exercise with CSPG degrading therapies (including ChABC [56, 57] or ADAMTS4 (a disintegrin and metalloproteinase with thrombospondin motifs 4) (Griffin et al., 2020)) lead to synergistic effects, even when applied at chronic time-points [57]. These reinforce the concept that multifactorial therapies are the way to go in order to tackle the different aspects of the pathophysiology of SCIs [59].

Although neither our experiments nor other studies [54], did not demonstrate the presence of an activity-triggered transcriptional switch, more chronic stimulations could be leading to it, although with our current knowledge, more local and transient cellular mechanisms seem responsible of the the growth differences observed with stimulation of activity specifically at a cellular level. For example, neuronal activity changes the excitability of neurons through reorganization of several ionic channels [41, 60, 61]. This can in turn influence growth, as a result of intracellular ionic adjustments and their downstream associated signalling [42, 62], or even translational changes [41]. Neuronal activity can also alter neuronal metabolism, increasing glycolysis, and lipid synthesis and integration to the membrane, a cellular process essential during axonal extension [63, 64]. Another important cellular component altered by activity is the cytoskeleton and its dynamics, for instance, neuronal activity has been shown to increase dendritic spine microtubule polymerization [65]. Accordingly, chemogenetic stimulation increases microtubule dynamics in the distal axonal portion, by reducing tubulin acetylation and increasing tyrosination in this region [54]. These mechanisms may not be exclusive, on the contrary, they are likely to take place all together facilitating activity-induced axonal growth.

On the other hand, success of activity-based therapies does not depend solely on the cellular effects of activity modulations, instead, these therapies, that target activity in a more general and chronic way (as different neurons or even circuits are stimulated simultaneously), benefit from a raised general excitability that seems to be ultimate the responsible for the plasticity and reorganization that leads to recovery [52]. In that direction, rehabilitation and electrical stimulation after injury promote the formation of new synapses in the spinal cord [49, 66], respiratory function recovery after optogenetic stimulation is also attributed to synaptic plasticity [67], and a recent study showing that rehabilitation together with electrochemical stimulation promotes recovery, is credited to cortico-reticulo-spinal circuit remodelling [68]. Additionally, sprouting of spared axons, instead of injured ones, is also responsible for recovery after exercise and/or electrical stimulation [17–19, 29, 30]. In agreement to that, success of these approaches is only significant in incomplete injuries, and greater as more tissue is spared. Incomplete injuries might also help explaining why in our model we did not observe recovery after optogenetic stimulation of the motor cortex while others did [69], as different spinal injuries were used. Compellingly, compression injury leaves more uninjured tissue and spinal tracts than our injury, that axotomizes all the dorsal tracts, including the main component of the CST in mice. Besides, complete injuries also present larger glial scars, and therefore greater accumulation of growth inhibitory molecules, which translates in larger distances and hurdles to overcome or bypass to achieve functional connections, together with a greater loss of intraspinal circuits.

These observations strengthen the view that current activity-based therapies stimulate plasticity on top of inducing regeneration in specifically stimulated neurons, but probably without inducing long-lasting cellular reprogramming. This plasticity results from activity-triggered local changes, therefore prolonged stimulations are more effective increasing growth or regeneration [52]. This is also evidenced by the presence of functional recovery after 12, but not after 4 weeks of chemogenetic

stimulation [54]. Therapeutically, holistic more unspecific approaches, have a more potent effect than cellular specific stimulations alone, as evidenced by enriched environment compared to chemogenetic stimulation, which presents a lower rate of regeneration [44]. Studies have also shown that this activity-induced plasticity can be accelerated and improved by linking the activation of different relays topographically in a system [53, 70, 71]. These systems are however more challenging to define underlying mechanisms and understand the true nature of the gains of these therapies.

Briefly, we found that specific cellular stimulation of neuronal activity induced axonal growth, but only in the absence of inhibitory substrates. Likewise, this approach seems to be therapeutically less efficient in enhancing recovery than other more chronic or general stimulations. This also suggests and strengthens the idea that activity-based therapies succeed because of local transient cellular changes coupled with neuronal plasticity, rather than resulting in a cellular reprogramming of growth capacities, and because of that, longer stimulation periods elicit more robust responses.

## Conclusions

## List of abbreviations

## Declarations

### *Ethics approval and consent to participate*

Not applicable

### *Consent for publication*

Not applicable

### *Availability of data and materials*

All data generated or analysed during this study are included in this published article or available from the corresponding author on reasonable request.

## Competing interests

The authors declare that they have no competing interests" in this section.

## *Funding*

This research was supported by HDAC3-EAE-SCI Project with ref. PID2020-119769RA-I00 from MCIN/ AEI /10.13039/501100011033 to AH and PRPSEM Project with ref. RTI2018-099773-B-I00 from MCINN/AEI/10.13039/501100011033/ FEDER “Una manera de hacer Europa”, the CERCA Programme, and the Commission for Universities and Research of the Department of Innovation, Universities, and Enterprise of the Generalitat de Catalunya (SGR2017-648) to JADR. The project leading to these results received funding from the María de Maeztu Unit of Excellence (Institute of Neurosciences, University of Barcelona) MDM-2017-0729 and Severo Ochoa Unit of Excellence (Institute of Bioengineering of Catalonia) CEX2018-000789-S from MCIN/AEI /10.13039/501100011033. FMV was supported by a fellowship from the “Ayudas para la Formación de Profesorado Universitario” (FPU16/03992) program, from the Spanish Ministry of Universities.

## *Authors' contributions*

FMV performed, designed experiments, performed data analysis, and wrote the manuscript; SMT performed and designed experiments and performed data analysis; JADR supervised experiments, provided experimental funds and edited the manuscript; AH performed, designed experiments, performed data analysis, provided experimental funds, and wrote the manuscript.

## *Acknowledgements*

The authors thank Miriam Segura-Feliu and Ana López-Mengual for their technical help.

## 1 References

1. Fitch MT, Silver J (2008) CNS injury, glial scars, and inflammation: Inhibitory extracellular matrices and regeneration failure. Experimental Neurology. https://doi.org/10.1016/j.expneurol.2007.05.014

2. Richardson PM, McGuinness UM, Aguayo AJ (1980) Axons from CNS neurones regenerate into PNS grafts. Nature. https://doi.org/10.1038/284264a0

3. Huebner EA, Strittmatter SM (2009) Axon regeneration in the peripheral and central nervous systems. Results and Problems in Cell Differentiation. https://doi.org/10.1007/400_2009_19

4. Cregg JM, DePaul MA, Filous AR, Lang BT, Tran A, Silver J (2014) Functional regeneration beyond the glial scar. Experimental Neurology. https://doi.org/10.1016/j.expneurol.2013.12.024

5. Jones LL, Sajed D, Tuszynski MH (2003) Axonal Regeneration through Regions of Chondroitin Sulfate Proteoglycan Deposition after Spinal Cord Injury: A Balance of Permissiveness and Inhibition. Journal of Neuroscience. https://doi.org/10.1523/jneurosci.23-28-09276.2003

6. Ohtake Y, Li S (2015) Molecular mechanisms of scar-sourced axon growth inhibitors. Brain Research. https://doi.org/10.1016/j.brainres.2014.08.064

7. Sami A, Selzer ME, Li S (2020) Advances in the Signaling Pathways Downstream of Glial-Scar Axon Growth Inhibitors. Frontiers in Cellular Neuroscience. https://doi.org/10.3389/fncel.2020.00174

554 8. Curcio M, Bradke F (2018) Axon Regeneration in the Central Nervous System: Facing the
555 Challenges from the Inside. Annual Review of Cell and Developmental Biology.
556 https://doi.org/10.1146/annurev-cellbio-100617-062508

557 9. Mahar M, Cavalli V (2018) Intrinsic mechanisms of neuronal axon regeneration. Nature
558 Reviews Neuroscience. https://doi.org/10.1038/s41583-018-0001-8

559 10. He Z, Jin Y (2016) Intrinsic Control of Axon Regeneration. Neuron.
560 https://doi.org/10.1016/j.neuron.2016.04.022

561 11. Anderson MA, O'Shea TM, Burda JE, et al (2018) Required growth facilitators propel axon
562 regeneration across complete spinal cord injury. Nature. https://doi.org/10.1038/s41586-018-
563 0467-6

564 12. Wu D, Klaw MC, Connors T, Kholodilov N, Burke RE, Tom VJ (2015) Expressing
565 constitutively active rheb in adult neurons after a complete spinal cord injury enhances axonal
566 regeneration beyond a chondroitinase-treated glial scar. Journal of Neuroscience.
567 https://doi.org/10.1523/JNEUROSCI.0719-15.2015

568 13. Arlotta P, Molyneaux BJ, Chen J, Inoue J, Kominami R, MacKlis JD (2005) Neuronal
569 subtype-specific genes that control corticospinal motor neuron development in vivo. Neuron
570 45:207–221

571 14. Friel KM, Williams PTJA, Serradj N, Chakrabarty S, Martin JH (2014) Activity-Based
572 Therapies for Repair of the Corticospinal System Injured during Development. Frontiers in
573 Neurology. https://doi.org/10.3389/fneur.2014.00229

574 15. Goganau I, Sandner B, Weidner N, Fouad K, Blesch A (2018) Depolarization and electrical
575 stimulation enhance in vitro and in vivo sensory axon growth after spinal cord injury.
576 Experimental Neurology 300:247–258

577 16. Udina E, Furey M, Busch S, Silver J, Gordon T, Fouad K (2008) Electrical stimulation of
578 intact peripheral sensory axons in rats promotes outgrowth of their central projections.
579 Experimental Neurology 210:238–247

580 17. Carmel JB, Kimura H, Berrol LJ, Martin JH (2013) Motor cortex electrical stimulation
581 promotes axon outgrowth to brain stem and spinal targets that control the forelimb impaired by
582 unilateral corticospinal injury. European Journal of Neuroscience 37:1090–1102

583 18. Carmel JB, Kimura H, Martin JH (2014) Electrical stimulation of motor cortex in the
584 uninjured hemisphere after chronic unilateral injury promotes recovery of skilled locomotion
585 through ipsilateral control. Journal of Neuroscience 34:462–466

586 19. Carmel JB, Berrol LJ, Brus-Ramer M, Martin JH (2010) Chronic electrical stimulation of the
587 intact corticospinal system after unilateral injury restores skilled locomotor control and
588 promotes spinal axon outgrowth. Journal of Neuroscience 30:10918–10926

589 20. Deisseroth K (2015) H I S TO R I C A L C O M M E N TA RY Optogenetics : 10 years of
590 microbial opsins in neuroscience. 18:1213–1225

591 21. Sternson SM, Roth BL (2014) Chemogenetic tools to interrogate brain functions. Annual
592 Review of Neuroscience 37:387–407

593 22. Arenkiel BR, Peca J, Davison IG, Feliciano C, Deisseroth K, Augustine GJJ, Ehlers MD, Feng
594 G (2007) In Vivo Light-Induced Activation of Neural Circuitry in Transgenic Mice Expressing
595 Channelrhodopsin-2. Neuron. https://doi.org/10.1016/j.neuron.2007.03.005

596 23. Sala-Jarque J, Mesquida-Veny F, Badiola-Mateos M, Samitier J, Hervera A, del Río JA (2020)
597 Neuromuscular Activity Induces Paracrine Signaling and Triggers Axonal Regrowth after
598 Injury in Microfluidic Lab-On-Chip Devices. Cells 9:302

599 24. Taylor AM, Blurton-Jones M, Rhee SW, Cribbs DH, Cotman CW, Jeon NL (2005) A
600 microfluidic culture platform for CNS axonal injury, regeneration and transport. Nature
601 Methods. https://doi.org/10.1038/nmeth777

602 25. Siegle JH, López AC, Patel YA, Abramov K, Ohayon S, Voigts J (2017) Open Ephys: An
603 open-source, plugin-based platform for multichannel electrophysiology. Journal of Neural
604 Engineering. https://doi.org/10.1088/1741-2552/aa5eea

605 26. Basso DM, Fisher LC, Anderson AJ, Jakeman LB, McTigue DM, Popovich PG (2006) Basso
606 mouse scale for locomotion detects differences in recovery after spinal cord injury in five
607 common mouse strains. Journal of Neurotrauma. https://doi.org/10.1089/neu.2006.23.635

608 27. Meijering E, Jacob M, Sarria JCF, Steiner P, Hirling H, Unser M (2004) Design and
609 Validation of a Tool for Neurite Tracing and Analysis in Fluorescence Microscopy Images.
610 Cytometry Part A. https://doi.org/10.1002/cyto.a.20022

611 28. Sánchez-Ventura J, Giménez-Llort L, Penas C, Udina E (2021) Voluntary wheel running
612 preserves lumbar perineuronal nets, enhances motor functions and prevents hyperreflexia after
613 spinal cord injury. Experimental Neurology. https://doi.org/10.1016/j.expneurol.2020.113533

614 29. Goldshmit Y, Lythgo N, Galea MP, Turnley AM (2008) Treadmill training after spinal cord
615 hemisection in mice promotes axonal sprouting and synapse formation and improves motor
616 recovery. Journal of Neurotrauma 25:449–465

617 30. Engesser-Cesar C, Ichiyama RM, Nefas AL, Hill MA, Edgerton VR, Cotman CW, Anderson
618 AJ (2007) Wheel running following spinal cord injury improves locomotor recovery and
619 stimulates serotonergic fiber growth. Eur J Neurosci 25:1931–1939

620 31. Carulli D, Foscarin S, Rossi F (2011) Activity-Dependent Plasticity and Gene Expression
621 Modifications in the Adult CNS. Frontiers in Molecular Neuroscience 4:1–12

622 32. Hogan MK, Hamilton GF, Horner PJ (2020) Neural Stimulation and Molecular Mechanisms
623 of Plasticity and Regeneration: A Review. Frontiers in Cellular Neuroscience 14:1–16

624 33. Jaiswal PB, English AW (2017) Chemogenetic enhancement of functional recovery after a
625 sciatic nerve injury. European Journal of Neuroscience 45:1252–1257

626 34. Ward PJ, Jones LN, Mulligan A, Goolsby W, Wilhelm JC, English AW (2016) Optically-
627 induced neuronal activity is sufficient to promote functional motor axon regeneration in vivo.
628 PLoS ONE 11:1–16

629 35. Park S, Koppes RA, Froriep UP, Jia X, Achyuta AKH, McLaughlin BL, Anikeeva P (2015)
630 Optogenetic control of nerve growth. Scientific Reports 5:1–9

631 36. Ward PJ, Clanton SL, English AW (2018) Optogenetically enhanced axon regeneration: motor
632 versus sensory neuron-specific stimulation. European Journal of Neuroscience.
633 https://doi.org/10.1111/ejn.13836

634 37. Tyssowski KM, DeStefino NR, Cho JH, et al (2018) Different Neuronal Activity Patterns
635 Induce Different Gene Expression Programs. Neuron 98:530-546.e11

636 38. Lee PR, Cohen JE, Iacobas DA, Iacobas S, Douglas Fields R (2017) Gene networks activated
637 by specific patterns of action potentials in dorsal root ganglia neurons. Scientific Reports 7:1–
638 14

639 39. Miyasaka Y, Yamamoto N (2021) Neuronal Activity Patterns Regulate Brain-Derived
640 Neurotrophic Factor Expression in Cortical Cells via Neuronal Circuits. Frontiers in
641 Neuroscience. https://doi.org/10.3389/fnins.2021.699583

642 40. Fauth M, Tetzlaff C (2016) Opposing effects of neuronal activity on structural plasticity.
643 Frontiers in Neuroanatomy 10:1–18

644 41. Enes J, Langwieser N, Ruschel J, et al (2010) Electrical activity suppresses axon growth
645 through Cav1.2 channels in adult primary sensory neurons. Current Biology 20:1154–1164

646 42. Tedeschi A, Dupraz S, Laskowski CJ, Xue J, Ulas T, Beyer M, Schultze JL, Bradke F (2016)
647 The Calcium Channel Subunit Alpha2delta2 Suppresses Axon Regeneration in the Adult CNS.
648 Neuron 92:419–434

649 43. Rost BR, Schneider-warme F, Schmitz D, Hegemann P (2017) Primer Optogenetic Tools for
650 Subcellular Applications in Neuroscience. Neuron 96:572–603

651 44. Hutson TH, Kathe C, Palmisano I, et al (2019) Cbp-dependent histone acetylation mediates
652 axon regeneration induced by environmental enrichment in rodent spinal cord injury models.
653 Science Translational Medicine. https://doi.org/10.1126/scitranslmed.aaw2064

654 45. Senger JLB, Verge VMK, Macandili HSJ, Olson JL, Chan KM, Webber CA (2018) Electrical
655 stimulation as a conditioning strategy for promoting and accelerating peripheral nerve
656 regeneration. Experimental Neurology 302:75–84

657 46. Ahlborn P, Schachner M, Irintchev A (2007) One hour electrical stimulation accelerates
658 functional recovery after femoral nerve repair. Experimental Neurology 208:137–144

659 47. Al-Majed AA, Siu LT, Gordon T (2004) Electrical stimulation accelerates and enhances
660 expression of regeneration-associated genes in regenerating rat femoral motoneurons. Cellular
661 and Molecular Neurobiology 24:379–402

662 48. Al-Majed AA, Brushart TM, Gordon T (2000) Electrical stimulation accelerates and increases
663 expression of BDNF and trkB mRNA in regenerating rat femoral motoneurons. Eur J Neurosci
664 12:4381–4390

665 49. Loy K, Schmalz A, Hoche T, Jacobi A, Kreutzfeldt M, Merkler D, Bareyre FM (2018)
666 Enhanced Voluntary Exercise Improves Functional Recovery following Spinal Cord Injury by
667 Impacting the Local Neuroglial Injury Response and Supporting the Rewiring of Supraspinal
668 Circuits. J Neurotrauma 35:294–2915

669 50. Bradbury EJ, Burnside ER (2019) Moving beyond the glial scar for spinal cord repair. Nature
670 Communications. https://doi.org/10.1038/s41467-019-11707-7

671 51. Mesquida-Veny F, del Río JA, Hervera A (2021) Macrophagic and microglial complexity after
672 neuronal injury. Progress in Neurobiology. https://doi.org/10.1016/j.pneurobio.2020.101970

673 52. Courtine G, Sofroniew M v. (2019) Spinal cord repair: advances in biology and technology.
674 Nature Medicine. https://doi.org/10.1038/s41591-019-0475-6

675 53. Wagner FB, Mignardot JB, le Goff-Mignardot CG, et al (2018) Targeted neurotechnology
676 restores walking in humans with spinal cord injury. Nature 563:65–93

677 54. Wu D, Jin Y, Shapiro TM, Hinduja A, Baas PW, Tom VJ (2020) Chronic neuronal activation
678 increases dynamic microtubules to enhance functional axon regeneration after dorsal root
679 crush injury. Nature Communications 11:1–16

680 55. Lim JHA, Stafford BK, Nguyen PL, Lien B V., Wang C, Zukor K, He Z, Huberman AD
681 (2016) Neural activity promotes long-distance, target-specific regeneration of adult retinal
682 axons. Nature Neuroscience 19:1073–1084

683 56. García-Alías G, Barkhuysen S, Buckle M, Fawcett JW (2009) Chondroitinase ABC treatment
684 opens a window of opportunity for task-specific rehabilitation. Nature Neuroscience 12:1145–
685 1151

686 57. Wang D, Ichiyama RM, Zhao R, Andrews MR, Fawcett JW (2011) Chondroitinase combined
687 with rehabilitation promotes recovery of forelimb function in rats with chronic spinal cord
688 injury. 31:9332–9344

689 58. Griffin JM, Fackelmeier B, Clemett CA, Fong DM, Mouravlev A, Young D, O'Carroll SJ
690 (2020) Astrocyte-selective AAV-ADAMTS4 gene therapy combined with hindlimb
691 rehabilitation promotes functional recovery after spinal cord injury. Experimental Neurology.
692 https://doi.org/10.1016/j.expneurol.2020.113232

693 59. Griffin JM, Bradke F (2020) Therapeutic repair for spinal cord injury: combinatory
694 approaches to address a multifaceted problem. EMBO Molecular Medicine 12:1–29

695 60. Misonou H, Mohapatra DP, Park EW, Leung V, Zhen D, Misonou K, Anderson AE, Trimmer
696 JS (2004) Regulation of ion channel localization and phosphorylation by neuronal activity.
697 Nature Neuroscience 7:711–718

698 61. Romer SH, Deardorff AS, Fyffe REW (2016) Activity-dependent redistribution of Kv2.1 ion
699 channels on rat spinal motoneurons. Physiological Reports 4:1–11

700 62. Shim S, Ming GL (2010) Roles of channels and receptors in the growth cone during PNS
701 axonal regeneration. Experimental Neurology 223:38–44

702 63. Bas-Orth C, Tan YW, Lau D, Bading H (2017) Synaptic activity drives a genomic program
703 that promotes a neuronal warburg effect. Journal of Biological Chemistry 292:5183–5194

704 64. Segarra-Mondejar M, Casellas-Díaz S, Ramiro-Pareta M, Müller-Sánchez C, Martorell-Riera
705 A, Hermelo I, Reina M, Aragonés J, Martínez-Estrada OM, Soriano FX (2018) Synaptic
706 activity-induced glycolysis facilitates membrane lipid provision and neurite outgrowth. The
707 EMBO Journal 37:1–16

708 65. Hu X, Viesselmann C, Nam S, Merriam E, Dent EW (2008) Activity-dependent dynamic
709 microtubule invasion of dendritic spines. Journal of Neuroscience 28:13094–13105

710 66. Eisdorfer JT, Smit RD, Keefe KM, Lemay MA, Smith GM, Spence AJ (2020) Epidural
711 Electrical Stimulation: A Review of Plasticity Mechanisms That Are Hypothesized to Underlie
712 Enhanced Recovery From Spinal Cord Injury With Stimulation. Frontiers in Molecular
713 Neuroscience 13:1–12

714 67. Alilain WJ, Li X, Horn KP, Dhingra R, Dick TE, Herlitze S, Silver J (2008) Light-induced
715 rescue of breathing after spinal cord injury. Journal of Neuroscience 28:11862–11870

716 68. Asboth L, Friedli L, Beauparlant J, et al (2018) Cortico-reticulo-spinal circuit reorganization
717 enables functional recovery after severe spinal cord contusion. Nat Neurosci 21:576–588

718 69. Deng WW, Wu GY, Min LX, Feng Z, Chen H, Tan ML, Sui JF, Liu HL, Hou JM (2021)
719 Optogenetic Neuronal Stimulation Promotes Functional Recovery After Spinal Cord Injury.
720 Frontiers in Neuroscience 15:1–10

721 70. McPherson JG, Miller RR, Perlmutter SI, Poo MM (2015) Targeted, activity-dependent spinal
722 stimulation produces long-lasting motor recovery in chronic cervical spinal cord injury. Proc
723 Natl Acad Sci U S A 112:12193–12198

724 71. Mishra AM, Pal A, Gupta D, Carmel JB (2017) Paired motor cortex and cervical epidural
725 electrical stimulation timed to converge in the spinal cord promotes lasting increases in motor
726 responses. Journal of Physiology 595:6953–6968

727

728 **2 Figure legends**

729 **Figure 1. Increased neuronal activity promotes neurite outgrowth.** A. Representative images of
730 c-Fos (red) and ChR2 (green) immunostaining. White arrows depict $ChR2^+$ neurons. Scale bar:
731 100µm. a. Higher magnification image of a stimulated neuron. ChR2 expression is mainly located in
732 the membrane of large-diameter neurons. Scale bar: 20µm. B. c-Fos expression in the nucleus is
733 increased just after optogenetic stimulation of Thy1-ChR2 DRG neurons (n=20-25 cells). MFI: mean
734 fluorescence intensity. a.u.: arbitrary units. Data are expressed as mean nuclear fluorescence
735 intensity±s.e.m. **$p < 0.01$ denotes significant differences in Student's t-Test. C. Stimulated neurons
736 presented significantly higher neurite lengths when compared to non-stimulated ones. Average
737 neurite length per neuron was determined at 24h *in vitro*. Data are expressed as mean±s.e.m. *$p <$
738 0.05 denotes significant differences in Student's t-Test. D. Representative images of Tuj-1 staining
739 used to analyze neurite length. Scale bar: 200µm.

740

741 **Figure 2. Chemogenetic stimulation induced PNS regeneration.** A. Chemogenetically stimulating
742 DRG neurons *in vitro* 6h after axotomy resulted in regeneration promotion. Data are expressed as the
743 mean percentage of infected regenerating axons compared to the total of infected axons reaching the
744 axonal compartment±s.e.m (n=7-8 axonal compartments). *$p < 0.05$ denotes significant differences
745 in Student's t-Test. B. Representative images of hM3Dq/mCherry$^+$ axons. Scale bar: 50µm. C. c-Fos
746 nuclear staining is observed in hM3Dq infected DRG neurons (white arrows) 1h after CNO injection,
747 but not in mCherry$^+$ DRG neurons after the same treatment. Scale bar: 25µm. D. Schematic timeline
748 of the experiment. E. The number of regenerating sensory axons (SCG-10$^+$) in stimulated nerves
749 (hM3Dq-CNO) is increased in all assessed distances compared to the non-stimulated (mCherry-
750 CNO) reaching statistical significance in long distances. Data are expressed as mean±s.e.m. at each
751 distance from the injury site (n=9 sciatic nerves). *$p < 0.05$ denotes significant differences in
752 ANOVA followed by Bonferroni test. F. SCG-10 immunostaining of mCherry or hM3Dq infected
753 sciatic nerves 24h after SNC. Dotted lines indicate the injury site. Scale bar: 200µm.

754 **Figure 3. Optogenetic stimulation of cortical neurons after axotomy.** A. Cortical neurons (Tuj-1)
755 express ChR2-eYFP after LV-ChR2 infection. White arrows in the high magnification image indicate
756 neuritic expression of ChR2. Scale bar: 250µm. B. Optogenetic stimulation increased the expression
757 of c-Fos in cortical neurons. Representative images of c-Fos (red) and ChR2 (green) immunostaining.
758 Scale bar: 20µm. C-D. Optogenetic stimulation of cortical neurons 30min after axotomy (B) resulted
759 in reduced axon regeneration, while delivering the stimulation 6h after axotomy (C) increased axon
760 regeneration. Individual ChR2$^+$ axon lengths were quantified (B: n=16 images; C: n=37-43 images).
761 Data are expressed as mean±s.e.m. ***$p < 0.001$ denotes significant differences in Student's t-Test;
762 **$p < 0.01$ denotes significant differences in Mann Whitney test. E. Optogenetic stimulation (Light)
763 of WT cortical neurons did not induce any changes in axonal regeneration. Total growth

764 area/microchannel was computed (n=7-8 images). Data are expressed as mean±s.e.m. F.
765 Representative images of GFP/YFP staining used to analyze axon regeneration when stimulation is
766 applied 6h after axotomy. Scale bar: 200μm.

767

768 **Figure 4 Increasing neuronal activity does not induce recovery after CNS injury.** A. Timeline
769 of the CST injury and stimulation experiments. B-C. % of missteps in the gridwalk test (B) (n=8-9
770 mice per group for each timepoint) and BMS score (C) (n=10 mice per group for each timepoint)
771 show no differences in sensorimotor recovery in stimulated Thy1-ChR2 (ChR2 Light) mice when
772 compared to non-stimulated (ChR2 No light) after CST injury. D. Timeline of the DCA and
773 stimulation experiments. E-F. Chemogenetically stimulated animals (hM3Dq-CNO) show similar
774 sensorimotor function recovery to non-stimulated ones (mCherry-CNO, mCherry-veh , hM3Dq-veh)
775 after DCA as seen by the gridwalk (E) (n=3-5 mice per group for each timepoint) and BMS (F) (n=5-
776 6 mice per group for each timepoint) tests. Represented data correspond to the BMS score and % of
777 missteps in the gridwalk. Data are expressed as mean±s.e.m. ANOVA followed by Bonferroni post-
778 hoctest.

779 **Figure 5. Neuronal activity induces growth but is not sufficient to overcome inhibitory**
780 **environments.** A. Neurite outgrowth was significantly increased in optogeneticallty stimulated DRG
781 neurons over growth-permissive substrates (LAM: laminin), but not over different concentrations (5,
782 10, 20 μg/ml) of non-permissive substrates (CSPGs). Average neurite length per neuron was
783 determined at 24h *in vitro*. Data are expressed as mean neurite length per cell±s.e.m (n=6-23 images).
784 **$p < 0.01$ denotes significant differences in ANOVA followed by Bonferroni test. B. Representative
785 images of Tuj-1 staining used to analyze neurite length. Scale bar: 200μm. C. Representative images
786 of traced (Dextran-Alexa594) CST and ChR2-YFP in stimulated and non-stimulated Thy1-ChR2

mice in spinal cord sections 500µm rostral to the lesion core. Scale bar: 100µm. c. Higher magnification images. White arrows indicate double-positive Dextran-Alexa 594/ChR2-YFP sprouted axons. Scale bar: 50µm. D. The number of double-positive Dextran-Alexa 594/ChR2-YFP sprouted axons in the grey matter as a normalized ratio of Dextran-Alexa 594-traced CST axons shows a significantly higher percentage of sprouted axons in stimulated animals at distances up to 400µm laterally and ventrally from CST. Data are expressed as mean±s.e.m. at each distance from the CST (n=4 mice) ***$p < 0.001$; **$p < 0.01$ denote significant differences in ANOVA followed by Bonferroni test.

**Supplementary Figure 1. AAV-mCherry and AAV-hM3Dq infection of DRG neurrons.** A. Images of mCherry expression in AAV-mCherry and AAV-hM3Dq infected DRG neurons 4-5 weeks after viral injection. Scale bar: 100µm. B. Large-diameter DRG neurons are preferentially infected. % of large-diameter (diameter >35µm) infected neurons was analyzed (n=7-9 DRGs). Data are expressed as mean±s.e.m. C. Both AAVs infect $NFH^+$ cells. Scale bar: 30µm.

**Supplementary Figure 2. ChR2 expression and growth after CST axotomy in Thy1-ChR2 mice.** A. While some layer II-III neurons express ChR2, expression is concentrated in layer V neurons. Scale bar: 100µm. B. Schematic representation of the quantification in C. The spinal cord was divided in grey matter and white matter for analysis. C. Tracer intensity quantification of injured stimulated and non-stimulated Thy1-ChR2 mice at 0,5mm pre-injury and post-injury. Optogenetic stimulation of the CST resulted in increased sprouting in the grey matter pre-injury, but not post-injury. a.u.: arbitrary units. Data are expressed as mean tracer intensity±s.e.m (n=5 spinal cords). **$p < 0.01$ denotes significant differences in Student's t-Test.

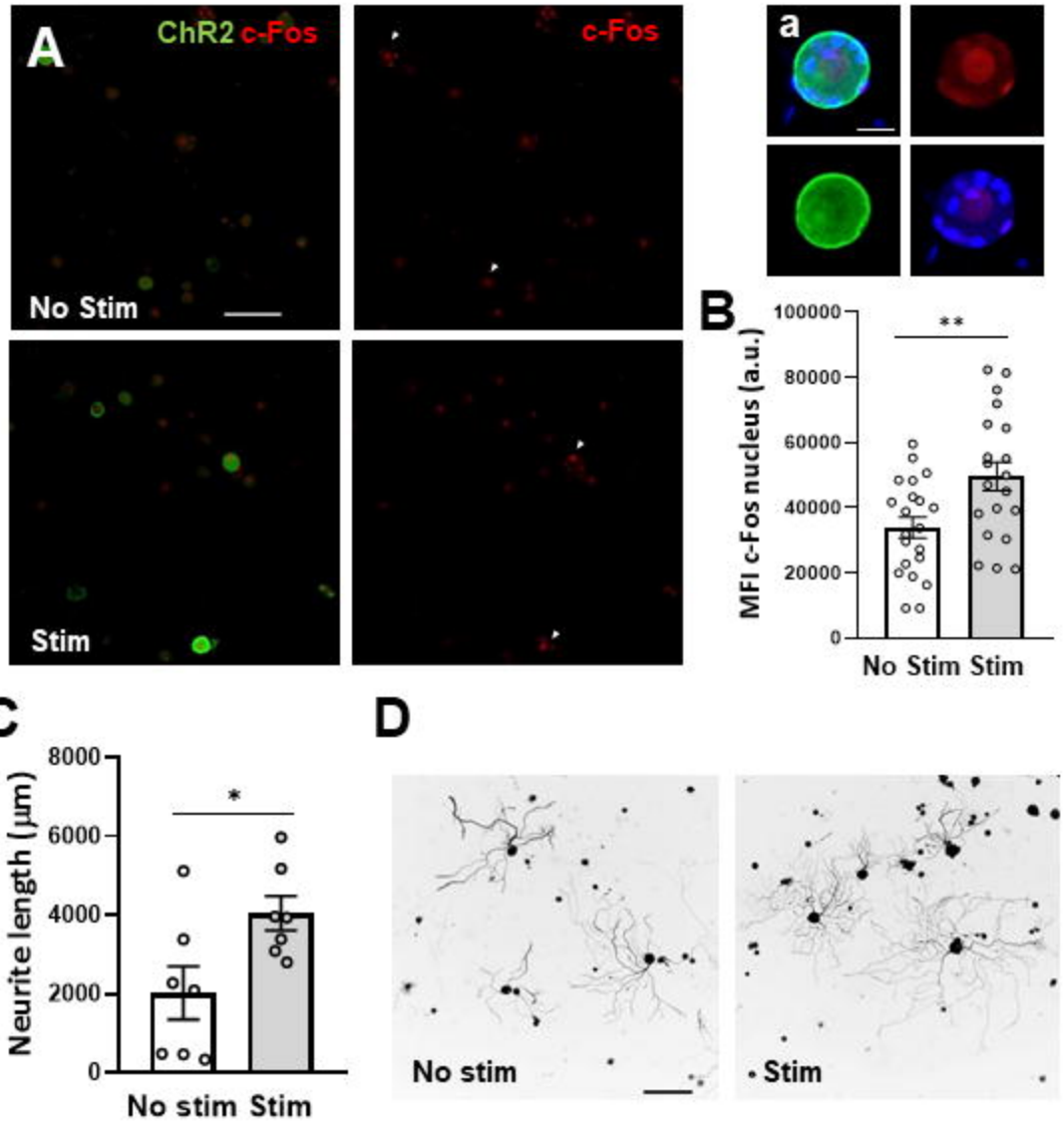
A
ChR2 c-Fos
c-Fos
No Stim
Stim
a
B
MFI c-Fos nucleus (a.u.)
100000
80000
60000
40000
20000
0
**
No Stim Stim
C
Neurite length (µm)
8000
6000
4000
2000
0
*
No stim Stim
D
No stim
Stim

Figure 1

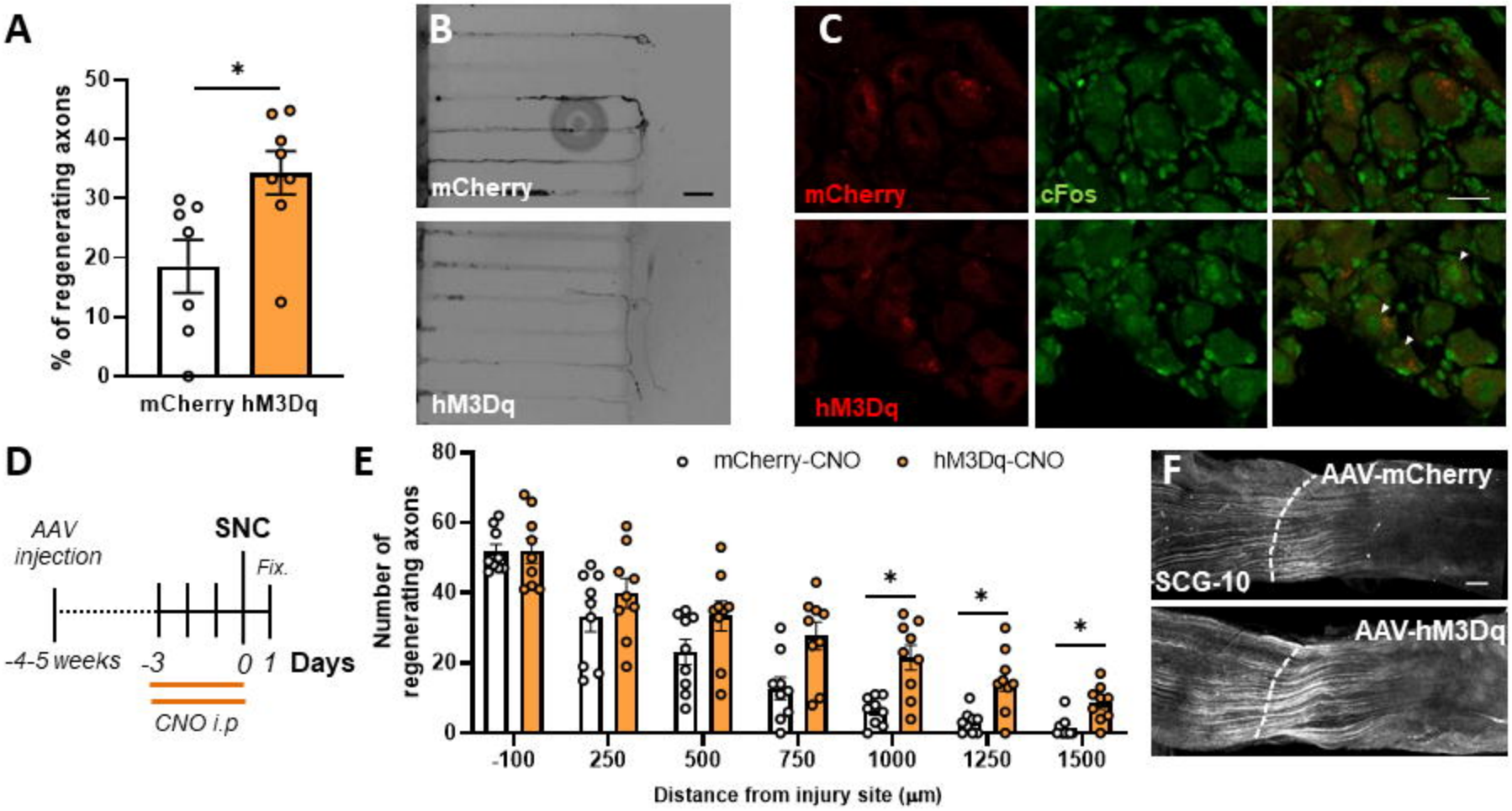
A
% of regenerating axons
50
40
30
20
10
0
*
mCherry hM3Dq
B
mCherry
hM3Dq
C
mCherry
cFos
hM3Dq
D
AAV injection
SNC
Fix.
-4-5 weeks
-3
0 1 Days
CNO i.p
E
mCherry-CNO
hM3Dq-CNO
Number of regenerating axons
80
60
40
20
0
-100
250
500
750
1000
1250
1500
Distance from injury site (µm)
F
AAV-mCherry
SCG-10
AAV-hM3Dq

Figure 2

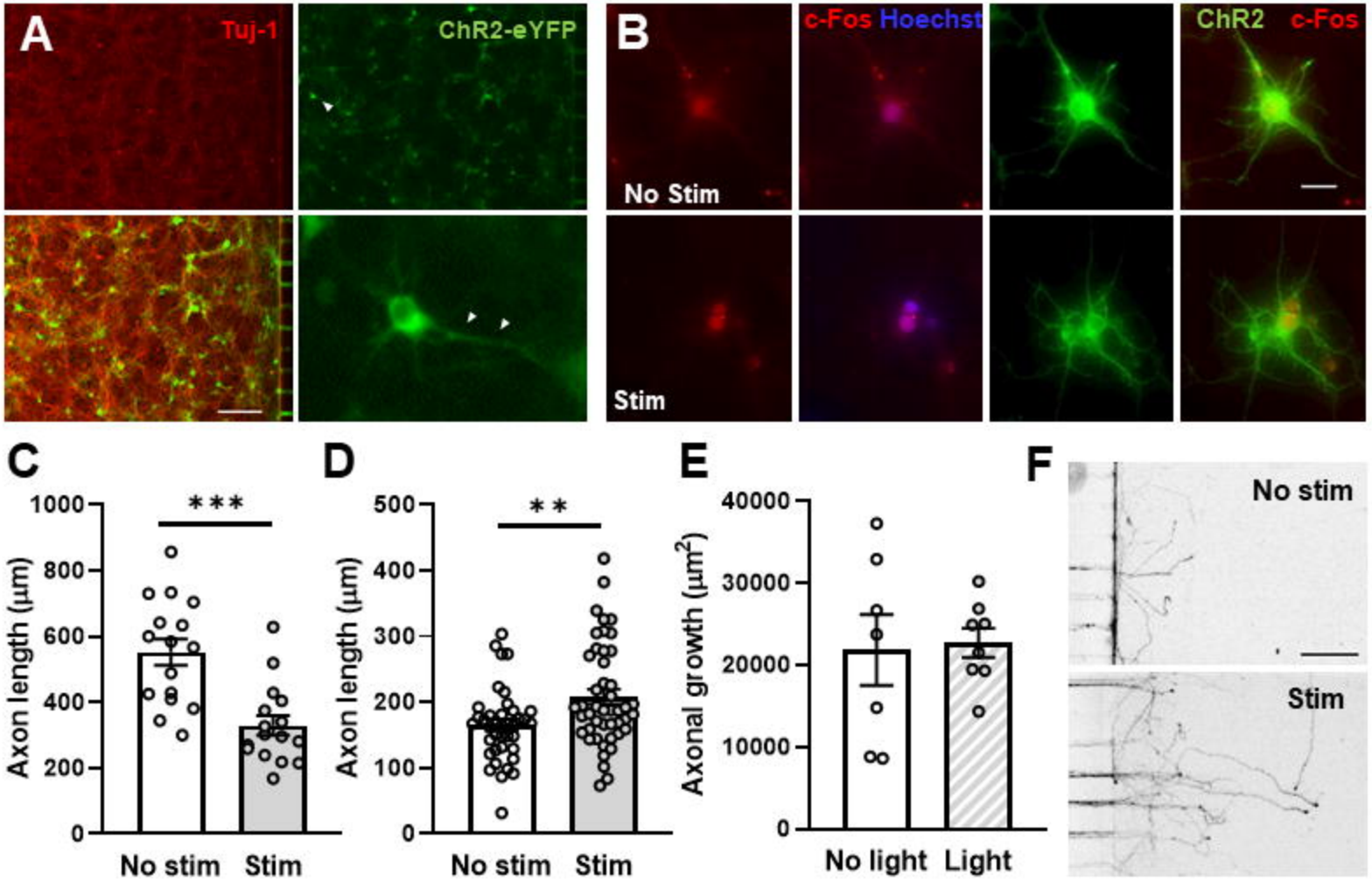
A
Tuj-1
ChR2-eYFP
B
c-Fos Hoechst
ChR2 c-Fos
No Stim
Stim
C
Axon length (µm)
1000
800
600
400
200
0
***
No stim
Stim
D
Axon length (µm)
500
400
300
200
100
0
**
No stim
Stim
E
Axonal growth (µm²)
40000
30000
20000
10000
0
No light
Light
F
No stim
Stim

Figure 3

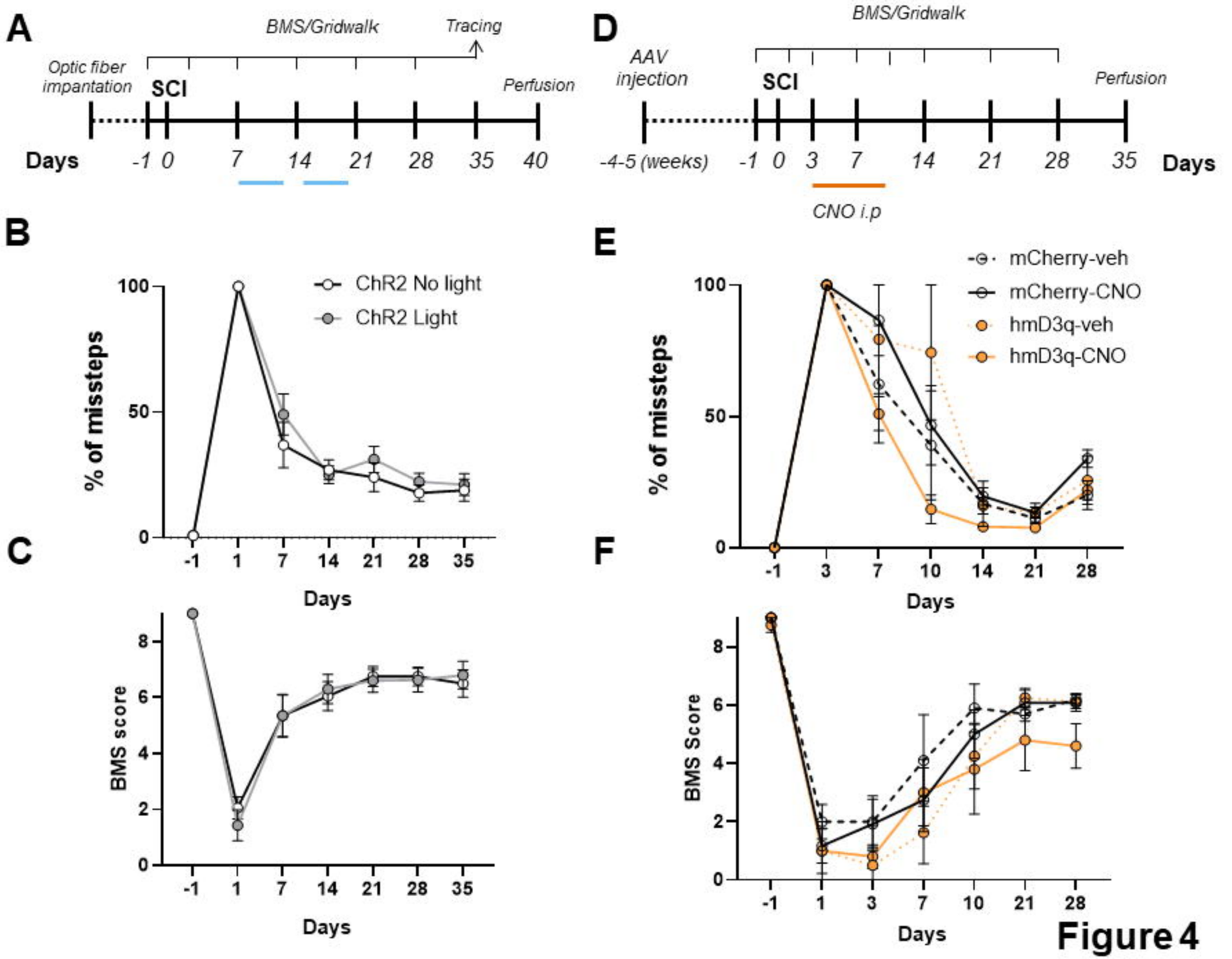
A
BMS/Gridwalk
Tracing
Optic fiber impantation
SCI
Perfusion
Days
-1 0 7 14 21 28 35 40
D
BMS/Gridwalk
AAV injection
SCI
Perfusion
-4-5 (weeks)
-1 0 3 7 14 21 28 35
Days
CNO i.p
B
ChR2 No light
ChR2 Light
% of missteps
100
50
0
-1 1 7 14 21 28 35
Days
C
BMS score
8
6
4
2
0
-1 1 7 14 21 28 35
Days
E
mCherry-veh
mCherry-CNO
hmD3q-veh
hmD3q-CNO
% of missteps
100
50
0
-1 3 7 10 14 21 28
Days
F
BMS Score
8
6
4
2
0
-1 1 3 7 10 21 28
Days

Figure 4

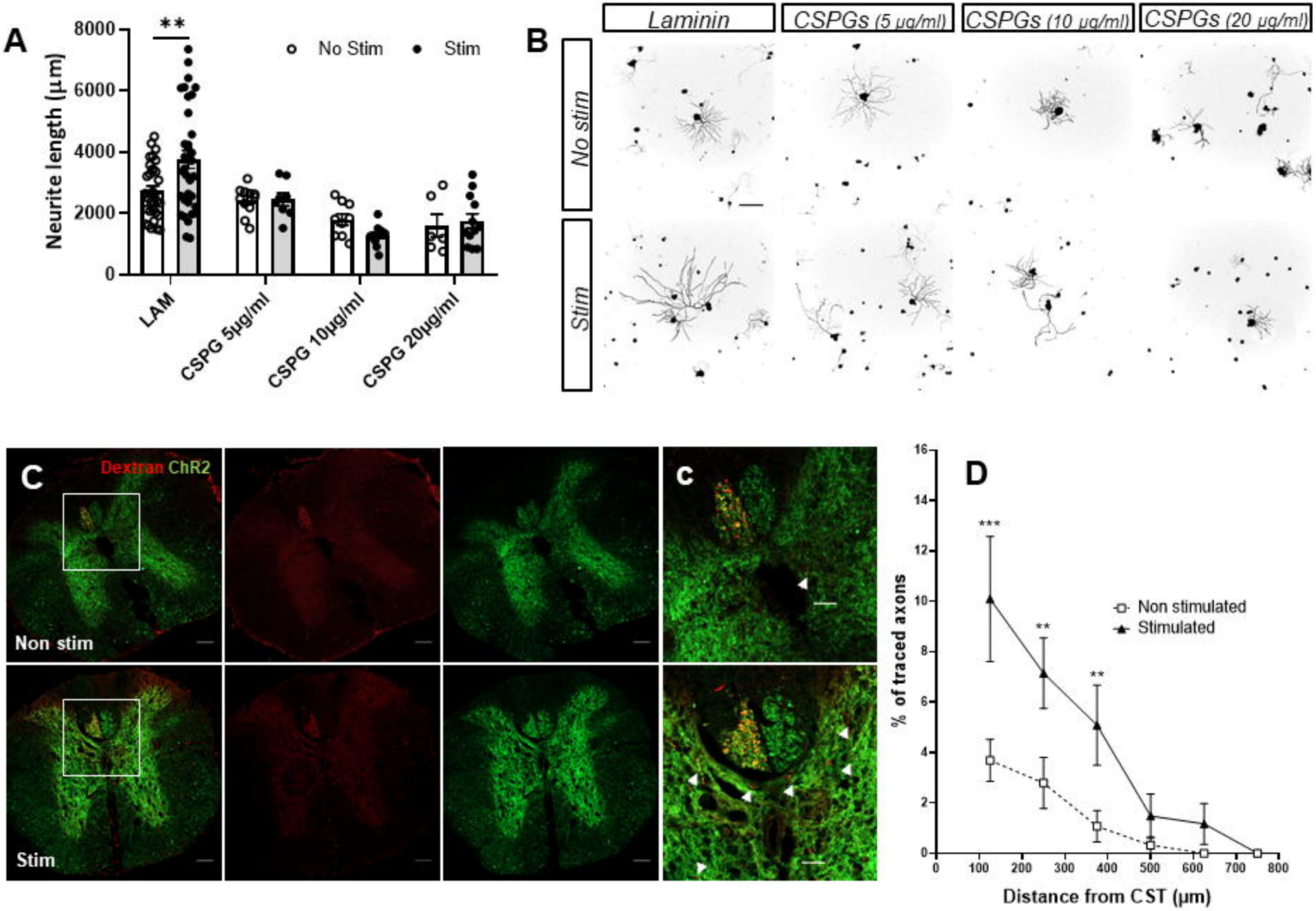
A
Neurite length (µm)
8000
6000
4000
2000
0
**
No Stim
Stim
LAM
CSPG 5µg/ml
CSPG 10µg/ml
CSPG 20µg/ml
B
Laminin
CSPGs (5 µg/ml)
CSPGs (10 µg/ml)
CSPGs (20 µg/ml)
No stim
Stim
C
Dextran ChR2
Non stim
Stim
c
D
% of traced axons
16
14
12
10
8
6
4
2
0
***
**
**
Non stimulated
Stimulated
0
100
200
300
400
500
600
700
800
Distance from CST (µm)

**Figure 5**